ANALYSIS OF USER TERMINAL TRADE-OFFS FOR FUTURE SATELLITE COMMUNICATION APPLICATIONS

Aparna P. T. Adithyababu, Federico Boulos, Stefano Caizzone
German Aerospace Center (DLR), Wessling, Germany,
aparna.parakkalthachappillyadithyababu@dlr.de, federico.boulos@dlr.de,
stefano.caizzone@dlr.de

Abstract

Despite the fact that ongoing advancements in telecommunication have led to 5th generation (5G) cellular networks, the increased demand for connectivity anywhere, at any time has highlighted the potential of a possible integration with non-terrestrial networks (NTNs). The 3rd generation partnership project (3GPP) defines NTN [1] as a network or segment of networks that uses space- or air-borne vehicles as relay nodes (transparent satellite architecture) or base stations (regenerative satellite architecture) to deliver service to users [2]. A communication satellite in Low-Earth Orbit (LEO), Medium-Earth Orbit (MEO), or Geostationary Earth Orbit (GEO) is referred to as a space-borne vehicle. Unmanned Aircraft System (UAS) including High-Altitude Platforms (HAPS) are examples of air-borne vehicles.

NTNs can complement 5G cellular networks with service continuity, ubiquity, and scalability [3], so that the users are able to connect to NTNs in accordance with their requirements when terrestrial networks are unavailable. Integration of 5G networks with GEO High throughput satellites (HTS) can improve the coverage and capacity in a large scale [4]. GEO satellites are at an altitude of about 35786 kilometers [3] above the equator. They also have longer service lives than the lower orbit satellites. Despite the fact that GEO satellites can provide global coverage with fewer satellites, they have a maximum one-way propagation delay of roughly 280 milliseconds [3]. This is considered a major drawback in using them for latency-critical applications (automation, gaming, video chats, etc.). As a result, over the last few years, there has been a surge in interest in MEO and LEO satellites over GEO satellites. MEO satellites orbit between 7000 and 25000 kilometers, while LEO satellites orbit between 300 and 1500 kilometers [3]. MEO and LEO satellites have a one-way propagation delay of 90 and 30 milliseconds, respectively [3]. They have more mobility and a smaller service area than GEO due to their close proximity to the earth. The deployment of a large network or constellation of satellites is required to achieve the desired global coverage [5]. These satellite constellations are viewed as a viable option to enhance 5G terrestrial networks since they promise great throughput and low latency [6]. The need for access anywhere anytime, however, necessitates the usage of customer or user terminals that can connect to these NTNs. The terminals must be able to maintain a continual link with the satellite in order to provide continuous connectivity. However, there are no universally recognized requirements for these user terminals, with the exception of International Telecommunication Union (ITU) (e.g. [7]) and European Telecommunications Standards Institute (ETSI) guidelines (e.g. [8]), which are naturally focused on ensuring interoperability with other systems rather than establishing performance requirements on the terminal itself. Therefore, the definition of the requirement has been left to the vendors, each trimming them to their system capability, with no clear picture of the boundaries of what is feasible. As a result, a detailed link budget analysis is required and will be performed in this paper to evaluate the feasibility and prospective usage for these communication systems, by analysing various possibilities and constraints for the customer terminals, such as size, weight, power, and cost (SWaP-C [9]) and observing the impact of those constraints on the achievable performance.

The mathematical model accounts for all gains and losses to determine the figures of merit defining the link's quality. As a result, this study gives a clearer picture of the trade-offs that must be made while addressing the market demands for compact and low-cost terminals.

1. Introduction

NTNs can complement 5G cellular networks with service continuity, ubiquity, and scalability. The goal of 5G wireless technology is to provide diverse services in the three usage scenarios defined by ITU: enhanced mobile broadband (eMBB), ultra-reliable and low-latency communications (URLLC), and

massive machine type communications (mMTC) [10]. The coverage of populated areas, rather than the coverage of geographical areas, motivates the deployment of terrestrial networks [3]. This results in geographical areas where access to 5G services via a terrestrial network's radio coverage is not possible. Apart from stationary users (or customers), a mobile user in terrestrial platforms (automobiles), aerial platforms, and maritime platforms may encounter situations where terrestrial networks do not provide the essential services continuously throughout their route. Furthermore, natural calamities such as floods or earthquakes might destroy the terrestrial network infrastructure. NTNs can be utilized for public safety, disaster recovery and associated emergency communication in such instances. When the terrestrial networks are overloaded, NTNs may also assist with traffic balancing. 3GPP defines these NTNs as a network or segment of networks that uses space- or air-borne vehicles to deliver service to the users [1].

Space-borne NTNs such as man-made satellites revolve around Earth in GEO, MEO, or LEO. Since the GEO satellites orbit synchronously with the Earth's rotation, they appear motionless for a ground observer. GEO satellites may not be able to ensure the required reliability and latency necessary for URLLC services (such as self-driving cars) because of their high altitude and significant propagation delays of about 280 milliseconds [3]. However, since they can provide global coverage with fewer satellites, they are considered ideal for broadcasting applications. MEO and LEO satellites orbit more closer to the Earth and, as a result, have shorter orbital periods than GEO. This indicates that to a user or spectator on the ground, the satellites appear to be moving. The low altitude and thus constrained field of view of LEO and MEO satellites make it necessary to employ a network (constellation) of satellites to provide worldwide coverage. Due to their reduced latency than GEO satellite communications, they also have a promising future in terms of improving coverage and capacity for technologies which are latency critical (such as self-driving cars). The complication lies with the user or customer terminal, which must be able to connect to the satellite in these orbits and maintain connectivity despite their relative motion. However, there are no universally recognized requirements for these user terminals, with the exception of ITU and ETSI guidelines, which are naturally focused on ensuring interoperability with other systems rather than establishing performance requirements on the terminal itself. Therefore, the definition of the requirement has been left to the vendors, each trimming them to their system capability, with no clear picture of the boundaries of what is feasible. In order to assess the viability and potential application of these communication systems, a thorough link budget analysis is necessary.

This paper presents a link budget analysis that is carried out to comprehend the user terminal characteristics and trade-offs in satellite communication applications. The analysis considers a variety of limitations for the customer terminals, such as the size, field of view etc. to see how these constraints affect the achievable performance. The terminal constraints and other factors affecting the link budget are explained in detail in Section 2. The results of numerical computations and simulations are shown in Section 3. Conclusions are drawn in Section 4.

2. Parameters influencing link budget analysis

To determine the performance of the satellite communication link, Carrier-to-Noise Ratio (C/N) was calculated for both forward downlink (from satellite to the terminal) and return uplink (from terminal to the satellite) components. However, a number of parameters, including the receiver's Gain/Temperature (G/T), the transmitter's Effective Isotropic Radiated Power ($EIRP$), Free Space Path Loss ($FSPL$), Atmospheric Loss (AL), carrier bandwidth (BW), etc., must be assumed or determined for the computations. The satellite serves as the transmitter and the antenna terminal as the receiver during the forward downlink (DL), whereas during the return uplink (UL), the satellite serves as the receiver and the terminal as the transmitter.

2.1 User terminal antenna

The boresight vector depicts the direction of the maximum radiation from an antenna. The gain in the direction of maximum radiation can be expressed generally as [5]

$$G_m[\text{dBi}] = 10\log\left(\frac{4\pi A_{eff}}{\lambda^2}\right) \quad (1)$$

where λ is the wavelength and A_{eff} is the effective aperture area of the antenna. The maximum effective area of a uniform array can be regarded as its physical area [11]. Therefore, given a rectangular array in the X-Y plane, the maximum effective area can be calculated as the product of the side lengths Lx and Ly. When the satellite position is not along the broadside direction (direction perpendicular to the surface) of the terminal, the beam needs to be pointed or steered to a scan angle θ to track the satellite. However, the gain decreases when the beam is pointed away from broadside. The reduced gain can be calculated as [5]

$$G[\text{dBi}] = G_m[\text{dBi}] + cr \times 10\log(\cos(\theta)) \tag{2}$$

where cr is the cosine roll-off value. The terminal's G/T in dB/K can be calculated as G[dBi]$-T$[dBK]. In order to calculate the G/T value of the terminal, the system temperature should be calculated. The system noise temperature includes the antenna noise, diplexer losses and the low noise block down converter (LNB) noises. The antenna noise temperature can be calculated as [5]

$$T_A[\text{K}] = \frac{T_{sky}}{A_{rain}} + T_m\left(1 - \frac{1}{A_{rain}}\right) + T_{ground} \tag{3}$$

where T_m is the mean thermodynamic temperature of 275 Kelvin, T_{sky} is the sky temperature, T_{ground} is the ground temperature, and A_{rain} is the attenuation due to rain. In this work, T_A was considered to be 170 Kelvin, which, when combined with a 0.15 dB diplexer loss and a 1 dB LNB noise figure, resulted a total temperature T of 256 Kelvin. The $EIRP$ of the antenna terminal can be expressed as [5]

$$EIRP[\text{dBW}] = P[\text{dBW}] + G[\text{dBi}] \tag{4}$$

where P is the input power given to the antenna.

2.2. Propagation medium

The reduction in strength of an electromagnetic signal as it travels through free space on a line-of-sight path from a transmitting antenna to a receiving antenna is known as free-space path loss ($FSPL$). The free space path loss can be computed as [12]

$$FSPL[\text{dB}] = 20log\ (d[\text{km}]) + 20log\ (f[\text{GHz}]) + 92.45 \tag{5}$$

where d is the slant range (distance between satellite and terminal) and f is the frequency. The slant range can be computed as [13]

$$d[\text{km}] = \sqrt{(R_e^2 \sin^2\epsilon + h^2 + 2hR_e)} - R_e sin\epsilon \tag{6}$$

where R_e is the Earth radius (6378 kilometers), ϵ is the elevation angle, and h is the orbital altitude of the satellite. Low elevation angles to the satellite implies a higher slant range. For $\epsilon = 90$ degrees, slant range equals the altitude h. Along with frequency, elevation angle, and altitude, other factors that affect wave propagation via the medium include water vapour density. The resulting atmospheric loss can be calculated as [13]

$$AL\ [\text{dB}] = \frac{A_{zenith}(f)}{\sin\epsilon} \tag{7}$$

where $A_{zenith}(f)$ is as given by ITU in [14]. In addition to the above listed factors, the rain attenuation, A_{rain}, is an additional loss or attenuation component to be considered. The ITU has split the world map into climatic zones ranging from A to Q [15]. To aid in the calculation, a rainfall rate R is assigned to these zones. The value of A_{rain} can be calculated as [5]

$$A_{rain}\ [\text{dBi}] = \gamma_R L_e \tag{8}$$

where γ_R is the specific attenuation depending on R and L_e is the slant range of the wave in rain. Although the link budget analysis in this paper is performed under clear sky condition, the rain attenuation was evaluated in order to better understand its influence on the signal. For a variable annual

percentage (p) during which R has surpassed, the techniques employed in [5] were applied to obtain the rain attenuation for zone H at 30GHz UL frequency. The results are displayed in Tab. 1.

p [%]	R (zone H) [mm/h]	A_{rain}[dB]
1	2	1.03
0.1	10	4.59
0.01	32	13.23

Tab. 1. Rain attenuation for Zone H.

As indicated by the results, the expected availability has a considerable impact on the carrier to noise ratio margin that should be allowed for rain fade. The margin is sensitive to the desired availability, set by the customer expectations.

2.3. Satellite

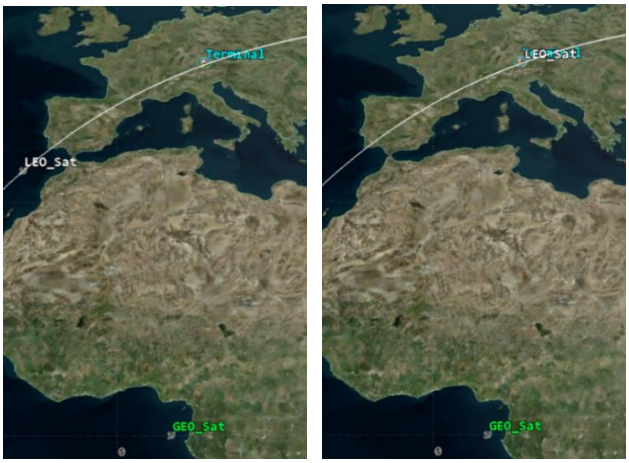

(a) (b)

Fig. 1. 2D graphic images showing positions of the satellites and terminal, LEO satellite moving from (a) ϵ~2.5° to (b) ϵ~88°.

Parameters	GEO scenario	LEO scenario
$EIRP$ [dBW]	54	39.4
G/T [dB/K]	7	9.8
h [km]	35787	590
ϵ [deg]	34.5	34.5
d [km]	38224	961

Tab. 2. Satellite reference values

The terminal was considered to be located at 48.08°N 11.29°E (German Aerospace Centre, Oberpfaffenhofen) and is denoted as 'Terminal' in Fig. 1. In order to calculate the link budget, satellite parameters such as $EIRP$, G/T, and slant range need to be known. The satellite reference values used for the calculation are listed in Tab. 2. Realistic values from known GEO (Eutelsat 7B [16]) and LEO (SpaceX Starlink [17]) satellites were used to obtain the numbers in Tab. 2. The LEO satellite, as

opposed to the GEO satellite, is moving with respect to the terminal, hence the elevation angle will change. Therefore, numerical calculations for LEO were done for ϵ = 34.5 degrees in order to provide a better comparison with GEO. The scenarios were simulated using Ansys System Tool Kit (STK) [18] in addition to the numerical calculations. Two of the time occurrences (about 6 minutes apart) captured in 2-D from the simulation are shown in Fig. 1.

3. Link budget analysis

To analyse the performance of the UL (30GHz) and DL (20GHz) communication links between the satellite and the terminal, Figure of Merits (FoM) such as C/N, spectral efficiency, and data rate were estimated. The carrier-to-noise ratio was computed as [5]

$$C/N\ [\text{dB}] = EIRP[\text{dBW}] - BW[\text{dBHz}] - FSPL[\text{dB}] - AL[\text{dB}] + \frac{G}{T}[\text{dB/K}] - k[\text{dBJ/K}] \quad (9)$$

where BW is the carrier bandwidth, k is the Boltzmann's constant (-228.6), and the remaining terms can be computed using (1-8). For a square array with sides of 0.3 meters and a cosine roll-off value of 1.2, the terminal parameters at broadside and scanning direction (scan angle $\theta = 90 - \epsilon$ =55.5°) were computed. Tab. 3 presents the outcome. The array's size (0.3 meters) was chosen in such a way that the resulting gain values were comparable to a known antenna terminal in [19].

Parameters	Broadside (θ =0°)	Scanning (θ =55.5°)
G [dBi]	37.0 (DL), 40.5 (UL)	34.0(DL), 37.5 (UL)
G/T [dB/K]	12.9	9.98
$EIRP$ [dBW]	45.9	43.0

Tab. 3. Calculated terminal parameters.

Fig. 2 shows the results of computing the gain reduction with varying scan angle using a cosine roll-off value of 1.2 in (2). Gain of the terminal falls with increasing scan angle (or decreasing elevation angle), which implies a declination in G/T and $EIRP$ values of the terminal.

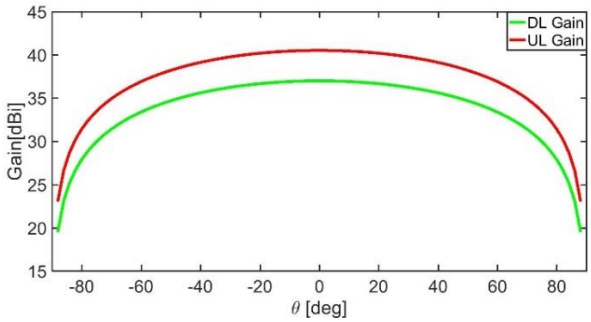

Fig. 2. Variation in gain w.r.t scan angle.

The spectral efficiency SE [bps/Hz] was calculated using the Shannon limit as $\log_2(1 + C/N)$. It is important to keep in mind that the commercially available modems have spectral efficiencies below the Shannon limit [12], which causes the predicted data rates in the paper to be larger than they are in reality. The data rate was computed as

$$Th[\text{Mbps}] = SE[\text{bps/Hz}] \times BW[\text{MHz}] \quad (10)$$

The calculated FoM are displayed in Tab. 4. The values in the Tab.4 corresponds to a DL and UL carrier bandwidth of 4 and 2 Megahertz. The values are calculated considering the user terminal pointing the beam at the satellite at 34.5° elevation (θ =90$-\epsilon$ =55.5°).

FoM	DL		UL	
	GEO	LEO	GEO	LEO
C/N [dB]	16.1	33.8	1.62	36.7
SE [bps/Hz]	5.38	11.2	1.29	12.2
Th [Mbps]	21.5	44.9	2.5	24.4

Tab. 4. Calculated FoM of the link.

It should be noted that the LEO satellite can deliver significantly better link performance than GEO satellite for a given antenna terminal and carrier bandwidth. Despite the fact that $EIRP$ for the GEO satellite is larger, its $FSPL$ is significantly higher, which yields a lower C/N value. According to (5), the elevation angle to the satellite and hence the scan angle of the terminal influences the resulting $FSPL$. For a better comprehension, the scenarios were simulated in STK over a time period represented in Fig. 1(a) to Fig. 1(b) to obtain Fig. 3 which shows the variation in the scan angle of the terminal.

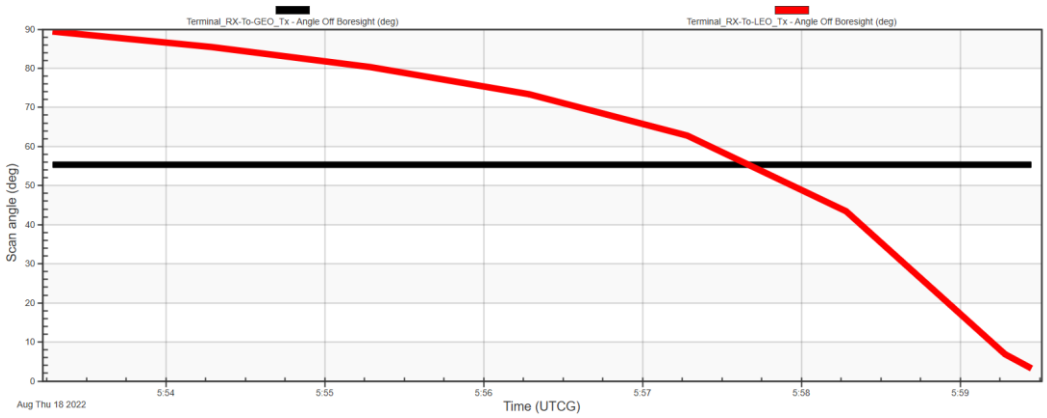

Fig. 3. Variation of the scan angle of LEO (red curve) and GEO (black curve) satellite w.r.t scenario time (duration ~ 6 minutes).

The scan angle stays constant at 55.5° for the GEO satellite fixed at 34.5° elevation. This results in a constant value for $FSPL$ and C/N for GEO as shown in Fig. 4 and Fig. 5. However, for LEO scenario, when the satellite approaches the terminal, the scan angle decreases. LEO satellite exhibits a reduced $FSPL$, which improves the C/N at a smaller scan angle. Additionally, it is to be noted that the simulated results concur with the numerical results (for DL) shown in Tab. 4 for θ =55.5°. The aforementioned observations lead to the conclusion that when designing the terminal, one should consider how the scan angle affects the G/T and $EIRP$ of the terminal, $FSPL$, and the resulting C/N values.

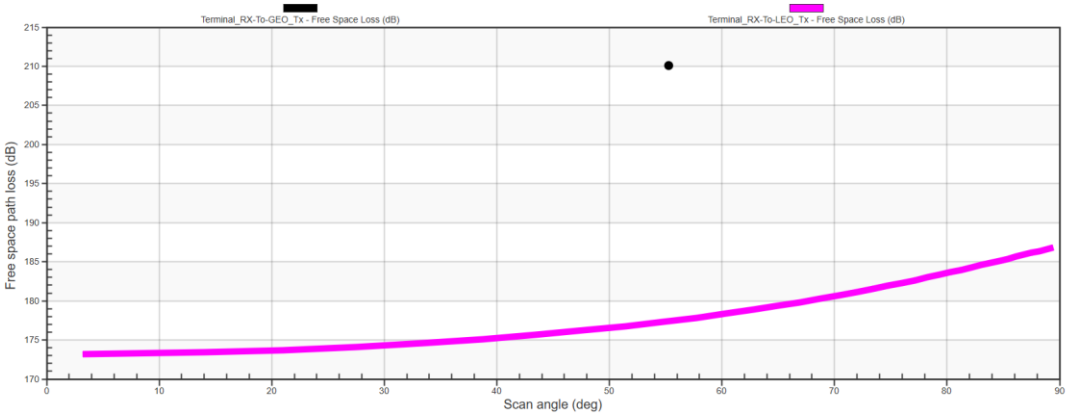

Fig. 4. Variation in DL $FSPL$ w.r.t θ for LEO (pink curve) and GEO (black marker) satellite.

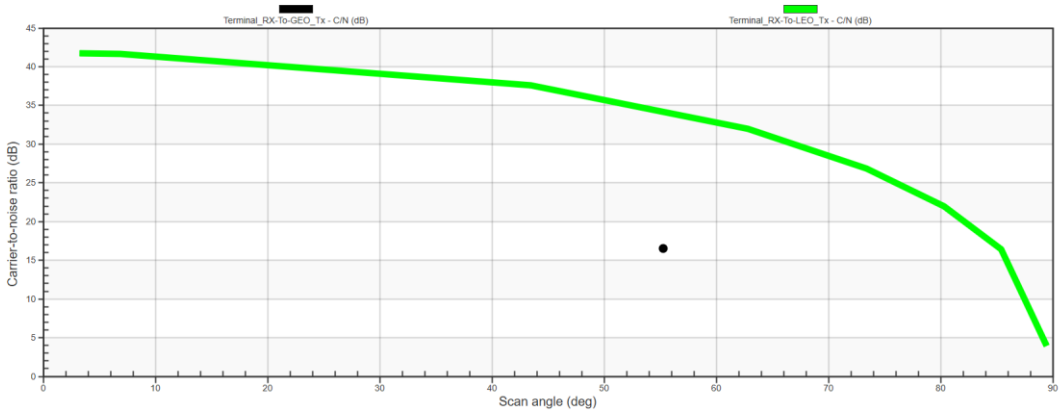

Fig. 5. Variation in DL C/N w.r.t θ for LEO (green curve) and GEO (black marker) satellite.

To improve the C/N and Th values of GEO (or LEO) scenario, one could increase the antenna terminal aperture area. According to (1) and (4), this would lead to a higher gain and thus a higher G/T and $EIRP$ for the terminal in the DL and UL computations, respectively. The impact of increasing aperture area on the resulting C/N and Th values (GEO DL scenario) are depicted in Fig. 6. Although increasing the antenna aperture area might be an option in situations like aircraft mounted terminals, the size of the antenna is restricted when installing it on platforms such as automobiles. These findings show that, compared to GEO satellites, LEO satellites can offer the required throughput with smaller antennas, but at the cost of greater complexity due to the need for beam steering.

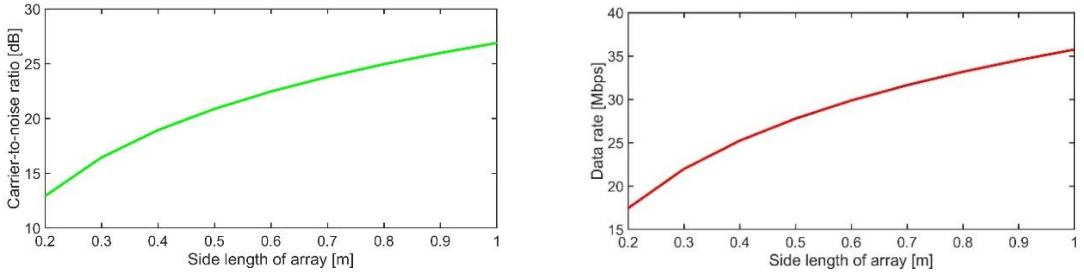

(a) (b)

Fig. 6. Variation in GEO DL (a) C/N and (b) Th w.r.t array size.

A different strategy to improve link performance from raising the aperture size is changing the carrier bandwidth (BW). Since the user can adjust the carrier bandwidth, the C/N values can change accordingly. The C/N will be improved as per (9) but the overall data rate is reduced when utilizing a smaller carrier band-width (as per (10)). This influence of the carrier bandwidth on C/N and Th (GEO DL scenario) is depicted in Fig. 7.

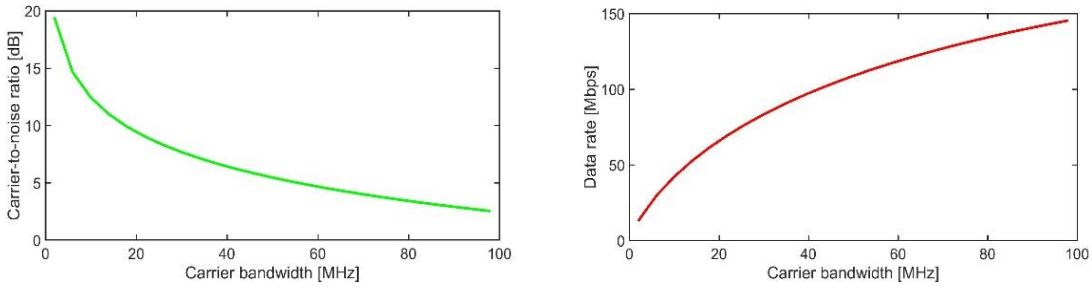

(a) (b)

Fig. 7. Variation in GEO DL (a) C/N and (b) Th for 0.3×0.3 m² array w.r.t BW.

It is recommended for the satellite-terminal communication link to have a high C/N for a better connectivity. However, there are scenarios where a high data rate is also necessary, such as a terminal fitted on a commercial aircraft with a significant number of passengers (users). In light of this, it is necessary to consider the impact of terminal parameters on the resulting communication link while evaluating the necessary size of the terminal to meet the market demands for a compact customer or user terminal.

4. Conclusion

In this paper, a link budget analysis was presented to understand the requirements on a user or customer terminal in satellite communication applications. As a result, it was made evident how the terminal parameters affect the performance of the link as well as any necessary compromises or trade-offs. When creating next-generation terminals, system engineers and antenna/user terminal architects can benefit from the offered study by having explicit rules and trade-offs, for example as the authors suggest in [9].

References

[1] *Solution for NR to support Non-Terrestrial Networks (NTN)*, 3GPP TR 38.821 V16.1.0, 2021.

[2] F. Rinaldi, H. -L. Maattanen, J. Torsner, S. Pizzi, S. Andreev, A. Lera, Y. Koucheryavy, and G. Araniti, “Non-terrestrial networks in 5G & beyond: A survey,” *IEEE Access*, vol. 8, 2020.

[3] *Study on using satellite access in 5G*, 3GPP TR 22.822 V16.0.0, 2018.

[4] O. Kodheli, A. Guidotti, and A. Vanelli-Coralli, “Integration of satellites in 5G through LEO constellations,” in *IEEE Global Communications Conference*, Singapore, Dec. 4-8, 2017, pp. 1-6.

[5] G. Maral and M. Bousquet, *Satellite Communications Systems*: *Systems, Techniques and Technology*, 3rd ed. Chichester, UK: Wiley, 1998.

[6] S. Liu, Z. Gao, Y. Wu, D. W. Kwan Ng, X. Gao, K. -K. Wong, S. Chatzinotas, and B. Ottersten, "LEO satellite constellations for 5G and beyond: How will they reshape vertical domains?," *IEEE Communications Magazine*, vol. 59, pp 30-36, Jul. 2021.

[7] *Reference radiation pattern for earth station antennas in the fixed-satellite service for use in coordination and interference assessment in the frequency range from 2 to 31 GHz*, Recommendation ITU-R S.465-6(01/2010), 2010.

[8] *Satellite Earth Stations and Systems (SES); Harmonised Standard for Earth Stations on Mobile Platforms (ESOMP) transmitting towards satellites in non-geostationary orbit, operating in the 27,5 GHz to 29,1 GHz and 29,5 GHz to 30,0 GHz frequency bands covering the essential requirements of article 3.2 of the Directive 2014/53/EU*, ETSI EN 303 979 V2.1.1 (2016-05), 2016.

[9] F. Boulos, S. Caizzone, and A. Winterstein, “A subarray-based antenna design for satellite communications ground terminals in Ka band,” in *26th Ka and Broadband Communications Conference*, Arlington, Virginia, USA, Sep. 27-30, 2021.

[10] *Minimum requirements related to technical performance for IMT-2020 radio interface(s)*, ITU-R M.2410-0, 2017.

[11] C. A. Balanis, *Antenna Theory: Analysis and Design*, 4th ed. Hoboken, NJ, USA: Wiley, 2016.

[12] “Link budget calculations for a satellite link with an electronically steerable antenna terminal,” Kymeta Corporation, White paper, Jun. 1, 2019. [Online]. Available: Link-Budget-Calculations-2.pdf (kymetacorp.com)

[13] *Study on new radio (NR) to support non-terrestrial networks,* 3GPP TR 38.811 V15.4.0, 2020.

[14] *Attenuation by atmospheric gases*, ITU-R P.676-10, 2013.

[15] *Characteristics of precipitation for propagation modelling*, ITU-R PN.837-1, 1994.

[16] “7° East satellites,” Eutelsat S. A., Paris, France. Accessed: Aug. 2, 2022. [Online]. Available: https://www.eutelsat.com/en/satellites/eutelsat-7-east.html

[17] A. Aguilar, P. Butler, J. Collins, M. Guerster, B. Kristinsson, P. Mckeen, K. Cahoy, E. Crawley, “Tradespace exploration of the next generation communication satellites,” in *AIAA SciTech*, San Diego, California, USA, Jan. 7-11, 2019.

[18] *Ansys System Tool Kit (STK) 12.5.0*. (2022). Analytical Graphics, Inc.

[19] “Request for experimental authorization,” Kuiper Systems LLC, Amazon, Nov. 1, 2021. [Online]. Available: https://apps.fcc.gov/els/GetAtt.html?id=285359&x=